Electronic Structure of the $[Fe_4Se_4]^{3+}$ Clusters in *C. vinosum* HiPIP and *Ectothiorhodospiza halophila* HiPIP II through NMR and EPR Studies

Ivano Bertini,*,† Stefano Ciurli,‡ Alexander Dikiy,† and Claudio Luchinat‡

Contribution from the Department of Chemistry, University of Florence, Via Gino Capponi, 7, 50121 Florence, Italy, and Institute of Agricultural Chemistry, University of Bologna, Viale Berti Pichat, 10, 40127, Bologna, Italy

Received June 22, 1993®

Abstract: The selenium-for-sulfur substitutions in the [4Fe–4S] core of the high-potential iron protein (HiPIP) from *Chromatium vinosum* and HiPIP II from *Ectothiorhodospiza halophila* were carried out, and the modified proteins were characterized by electronic EPR and NMR spectroscopies. EPR spectra showed a small increase in anisotropy and average g values. These results were interpreted as an indication that the Se-for-S substitution does not influence significantly the properties of the spin ground state. The assignment of the hyperfine shifted signals corresponding to protons of the four cysteine residues bound to the iron ions of the [4Fe–4Se] core was performed for both proteins using difference NOE, NOESY, EXSY, and TOCSY ^{1}H NMR methods. The changes induced by Se-for-S substitution on the magnetic coupling constants operative within the cluster core were inferred from the temperature dependence behavior of the paramagnetically shifted signals using a simple Heisenberg exchange model. The experimental data could be interpreted using a $J(Se) \cong 0.8J(S)$ and an overall decrease of J_{ij}, which seems to be more pronounced on the "mixed-valence" pair. This suggests a relative increase of the importance of double exchange on the "mixed-valence" pair upon Se-for-S substitution. Finally, the electronic distribution within the cluster core of HiPIP II from *E. halophila* was not modified by the presence of Se instead of S, whereas in HiPIP from *C. vinosum* a slight curvature of the temperature dependence of hyperfine shifted signals was interpreted as a further indication that an equilibrium exists between two orientations of the "ferric" and "mixed-valence" pairs within the cluster core.

Introduction

HiPIPs are a small class of iron–sulfur proteins, found in photosynthetic bacteria[1] and containing one [4Fe–4S] cluster,[2] which are able to exchange electrons at a relatively high potential.[3] The overall core charge changes between 2+ and 3+,[4] and the oxidized cluster contains formally three iron(III) and one iron(II). The outer shell electrons are distributed, within the cluster core, according to a scheme, derived from Mössbauer studies, which is consistent with the presence of a more reduced, so-called "mixed-valence" pair and of a less reduced, so-called "ferric" pair.[5-9] These two pairs are antiferromagnetically coupled to give an $S = {}^1/_2$ spin ground state.[8] Within this rather symmetric frame of interaction, the "mixed-valence" pair subspin S_{34} is larger than the "ferric" pair subspin S_{12}[8] (here 1–4 label the iron ions), and the most probable values of $|S_{34},S_{12}\rangle$ are $|^9/_2,4\rangle$ and $|^7/_2,3\rangle$.[9-16]

The above magnetic coupling scheme has been proposed to explain the ^{1}H NMR temperature-dependence behavior of the hyperfine shifted signals of oxidized native HiPIP[10-15] in terms of the expectation values $\langle S_{iz}\rangle$ of each metal ion i. The energy levels of the coupled system are given by

$$E = {}^1/_2[JS(S+1) + \Delta J_{12}S_{12}(S_{12}+1) + \Delta J_{34}S_{34}(S_{34}+1)] \pm B_{34}(S_{34}+{}^1/_2) \quad (1)$$

where J is the magnetic coupling constant for all the six possible pairs of iron ions, $J_{12} = J + \Delta J_{12}$, and $J_{34} = J + \Delta J_{34}$. The double-exchange term $\pm B_{34}(S_{34} + {}^1/_2)$ in practice has a similar effect on the $\langle S_{iz}\rangle$ values as the ΔJ_{34} term. Calculations are usually performed by omitting one of the two terms. When the double exchange term is omitted, a negative value of ΔJ_{34}[11-15] takes phenomenologically into consideration the contribution due to a double-exchange term in the "mixed-valence" pair.[10,17-25] This general scheme is able to qualitatively account for the shift

† University of Florence.
‡ University of Bologna.
® Abstract published in *Advance ACS Abstracts*, November 1, 1993.

(1) Bartsch, R. G. *Meth. Enzymol.* **1978**, *53*, 329–340.
(2) Carter, C. W., Jr. *Iron-Sulfur Proteins*; Academic Press: New York, 1977.
(3) Meyer, T. E.; Przysiecki, C. T.; Watkins, J. A.; Bhattacharyya, A.; Simondsen, R. P.; Cusanovich, M. A.; Tollin, G. *Proc. Natl. Acad. Sci. U.S.A.* **1983**, *80*, 6740–6744.
(4) Carter, C. W., Jr.; Kraut, J.; Freer, S. T.; Alden, R. A.; Sieker, L. C.; Adman, E. T.; Jensen, L. H. *Proc. Natl. Acad. Sci. U.S.A.* **1972**, *69*, 3526–3529.
(5) Moss, T. H.; Bearden, A. J.; Bartsch, R. G.; Cusanovich, M. A.; San Pietro, A. *Biochemistry* **1968**, *7*, 1591–1596.
(6) Evans, M. C. W.; Hall, D. O.; Johnson, C. E. *Biochem. J.* **1970**, *119*, 289–291.
(7) Dickson, D. P. E.; Johnson, C. E.; Cammack, R.; Evans, M. C. W.; Hall, D. O.; Kao, K.K. *Biochem. J.* **1974**, *139*, 105–108.
(8) Middleton, P.; Dickson, D. P. E.; Johnson, C. E.; Rush, J. D. *Eur. J. Biochem.* **1980**, *104*, 289–296.
(9) Bertini, I.; Campos, A. P.; Luchinat, C. Teixeira, M. *J. Inorg. Biochem.*, in press.
(10) Noodleman, L. *Inorg. Chem.* **1988**, *27*, 3677–3679.
(11) Banci, L.; Bertini, I.; Luchinat, C. *Struct. Bonding (Berlin)* **1990**, *72*, 113–135.
(12) Banci, L.; Bertini, I.; Briganti, F.; Luchinat, C.; Scozzafava, A.; Vicens Oliver, M. *Inorg. Chem.* **1991**, *30*, 4517–4524.
(13) Banci, L.; Bertini, I.; Briganti, F.; Luchinat, C. *New J. Chem.* **1991**, *15*, 467–477.
(14) Bertini, I.; Briganti, F.; Luchinat, C.; Scozzafava, A.; Sola, M. *J. Am. Chem. Soc.* **1991**, *113*, 1237–1245.
(15) Luchinat, C.; Ciurli, S. NMR of Polymetallic Systems in Proteins. In *Biological Magnetic Resonance*; Berliner, L. J., Reuben, J., Eds.; Plenum Press: New York, 1993, 357–420.
(16) Mouesca, J. M.; Lamotte, B.; Rius, G. *J. Inorg. Biochem.* **1991**, *43*, 251.
(17) Munck, E.; Papaefthymiou, V.; Surerus, K. K.; Girerd, J.-J. In *Metal Clusters in Proteins*; Que, L., Jr., Ed.; American Chemical Society: Washington, DC, 1988; pp 302–325.
(18) Borsch, S. A.; Chibotaru, L. F. *Chem. Phys.* **1989**, *135*, 375–380.
(19) Blondin, G.; Girerd, J.-J. *Chem. Rev.* **1990**, *90*, 1359–1376.
(20) Girerd, J.-J. *J. Chem. Phys.* **1983**, *79*, 1776–1781.
(21) Papaefthymiou, V.; Girerd, J.-J.; Moura, I.; Moura, J. J. G.; Munck, E. *J. Am. Chem. Soc.* **1987**, *109*, 4703–4710.
(22) Jordanov, J.; Roth, E. K. H.; Fries, P. H.; Noodleman, L. *Inorg. Chem.* **1990**, *29*, 4288–4292.
(23) Noodleman, L. *Inorg. Chem.* **1991**, *30*, 256–264.

0002-7863/93/1515-12020$04.00/0 © 1993 American Chemical Society

values and the temperature dependence of the β-CH_2 signals in the native oxidized HiPIPs from a number of sources.[12,14,26-32] Moreover, this model has allowed us to distinguish the temperature dependence behavior of the signals corresponding to the β-CH_2 protons of the cysteines bound to the "ferric" pair and to the "mixed-valence" pair.[11-15] In fact, according to this model, signals shifting upfield with increasing temperature correspond to the β-CH_2 of cysteine residues bound to the "mixed-valence" pair, whereas signals shifting downfield with increasing temperature correspond to the β-CH_2 of cysteine residues bound to the "ferric" pair. In this class of proteins, signals shifting upfield with increasing temperature are usually termed "Curie"-type signals, whereas signals shifting downfield with increasing temperature are termed "anti-Curie"- or "pseudo-Curie"-type signals, depending on their being downfield or upfield with respect to a diamagnetic reference. The valence-specific, sequence-specific assignment of a series of HiPIPs purified from several microorganisms has then been performed, thus identifying the cysteines bound to the "mixed-valence" and to the "ferric" pair.[26-32] We have concluded that two main locations of these pairs exist in the rigid asymmetric frame of the proteins, and we have proposed that an equilibrium may be present between two species differing for the valence distribution within the protein.[31,32]

The cluster contained in the native HiPIP from *C. vinosum* can be substituted with a cluster containing selenium instead of sulfur.[33a,34] We have prepared and investigated the selenium derivative of HIPIP II from *Ectothiorhodospiza halophila*, together with the selenium-substituted HiPIP from *Chromatium vinosum*, with the goal of better understanding the electronic structure of these systems and, in particular, the effect of Se substitution on the exchange parameters. Moreover, the effect of Se substitution will be discussed in the frame of the hypothesis[31,32] of the presence of the equilibrium between two different pairing schemes. For convenience, the following numbering scheme will be used throughout the paper: (**1**) native *E. halophila* HiPIP II, (**2**) native *C. vinosum* HiPIP, (**3**) selenium-substituted *E. halophila* HiPIP II, and (**4**) selenium-substituted *C. vinosum* HiPIP.

Experimental Section

All chemicals used were of the best quality available. Compounds **1**[30,35] and **2**[1] were purified according to previously reported procedures.

The selenium substitutions in the native proteins were performed using a scheme previously reported.[34,36] The detailed procedure for **3** has never been described and is given below.

All operations were carried out at 4 °C. A solution of 32% trichloroacetic acid (1 mL) was added dropwise to a sample of **1** (15 mg, 1.5×10^{-3} mmol) in 1 mL of 0.1 M Tris·HCl buffer at pH 7.8. The reddish-brown protein solution rapidly discolored, and the suspension of white apoprotein was stirred under nitrogen flow for 30 min to eliminate hydrogen sulfide and to bring the reaction of cluster disruption to completion. The precipitate was centrifuged and washed twice with trichloroacetic acid (5%). The apoprotein obtained was dissolved in 0.1 M Tris·HCl buffer at pH 9.0 (4 mL) and dialyzed for 2 h against 1 L of 0.1 M Tris·HCl at pH 7.8. All the following operations were carried out under nitrogen. A 0.1 M solution of dithiothreitol (1.5 mL, 0.15 mmol, 100-fold excess) was added to the dialyzed apoprotein solution, left stirring for 30 min, and subsequently, a 0.02 M solution of $FeCl_3$ (2 mL, 0.04 mmol, 25-fold excess) and a 0.01 M solution of Se^{2-} (6 mL, 0.06 mmol, 40-fold excess) (freshly prepared by adding 6 mL of a 0.1 M solution of dithiothreitol to 12 mg of Na_2SeO_3) were added. After 1 h, the final dark mixture was loaded onto a Whatman DE-52 column equilibrated with phosphate buffer, 20 mM, pH 7.5, 140 mM in NaCl, and the seleniated protein was eluted using the same buffer, 350 mM in NaCl. A black band remained at the top of the column, while ferric chloride and Fe_4Se_4–protein were subsequently eluted. The fractions containing the green-brown seleniated protein were collected and dialyzed overnight against 0.1 M phosphate buffer, pH 7.5. The protein thus obtained was in the oxidized form. A final purification of **3** was achieved by a further ion-exchange chromatography on a Whatman DE-52 column, using 10 mM phosphate buffer and a 0–400 mM NaCl gradient. The purity of **3** and **4** was checked by gel electrophoresis.

Samples for NMR spectroscopy were prepared using five cycles of deuterated buffer exchange (P_i 30 mM, pH* 5.2 (uncorrected for isotope effect) for **3**, and P_i 30 mM, pH* 7.15 for **4**) with an ultrafiltration Amicon cell equipped with a YM1 membrane. Samples for EPR spectroscopy were the same as those used for NMR. Reduction of **3** was performed by adding a few crystals of sodium dithionite to the oxidized protein, whereas oxidation of **4** was performed by adding a solution of potassium ferricyanide to the reduced protein. The extent of reduction and oxidation was established by ^1H NMR.

^1H NMR spectra were recorded with an AMX 600 Bruker spectrometer operating at 600.14-MHz Larmor frequency. The spectra were calibrated assigning a shift of 4.81 ppm, with respect to DSS, to the residual HOD signal at 298 K. A temperature dependence of the HOD signal was established, in the range of temperatures explored, and the following empirical relationship was found:

$$\mathrm{HOD(ppm)} = -0.012\ ^\circ\mathrm{C} + 5.11$$

X-band EPR spectra were recorded at 4 K with a Bruker ER-200-D SRC spectrometer operating at a microwave frequency of 9.44 GHz and equipped with a continuos-flow helium cryostat from Oxford Instruments. The spectra were calibrated assigning $g = 2.0037$ to the signal of solid DPPH.

UV–vis spectra were recorded using a Cary 3 UV–vis spectrophotometer.

CD visible spectra were recorded with a Jasco J-500C spectropolarimeter.

1D NOE difference spectra were accumulated using earlier described methodology.[37,38] The residual water signal was suppressed by using the Superweft[41] pulse sequence 180–τ–90–AQ, where τ and recycle time were varied between 60 and 130 ms and between 90 and 150 ms, respectively.

T_1 values were measured by the inversion–recovery method.[40]

1D saturation transfer experiments were performed as previously described.[14,41]

All 2D experiments were carried out in the phase sensitive mode. NOESY spectra[42-45] were recorded using the standard pulse sequence RD–90–t_1–90–t_m–90–AQ. Spectra were acquired with 512 experiments in the f_1 dimension, 128 scans per each experiment, and 1K data points in the f_2 dimension. Mixing and repetition times were 100 and 600 ms,

(24) Noodleman, L. *Inorg. Chem.* **1991**, *30*, 246–256.
(25) Blondin, G.; Borsch, S. A.; Girerd, J.-J. *Comments Inorg. Chem.* **1992**, *12*, 315–340.
(26) Bertini, I.; Capozzi, F.; Ciurli, S.; Luchinat, C.; Messori, L.; Piccioli, M. *J. Am. Chem. Soc.* **1992**, *114*, 3332–3340.
(27) Nettesheim, D. G.; Harder, S. R.; Feinberg, B. A.; Otvos, J. D. *Biochemistry* **1992**, *31*, 1234–1244.
(28) Bertini, I.; Capozzi, F.; Luchinat, C.; Piccioli, M.; Vicens Oliver, M. *Inorg. Chim. Acta* **1992**, *198-200*, 483–491.
(29) Bertini, I.; Capozzi, F.; Luchinat, C.; Piccioli, M. *Eur. J. Biochem.* **1993**, *212*, 69–78.
(30) Banci, L.; Bertini, I.; Capozzi, F.; Carloni, P.; Ciurli, S.; Luchinat, C.; Piccioli, M. *J. Am. Chem. Soc.* **1993**, *115*, 3431–3440.
(31) Banci, L.; Bertini, I.; Ciurli, S.; Ferretti, S.; Luchinat, C.; Piccioli, M. *Biochemistry*, in press.
(32) Banci, L.; Bertini, I.; Ferretti, S.; Luchinat, C.; Piccioli, M. *J. Mol. Struct.* **1993**, *292*, 207–220.
(33) (a) Moulis, J.-M.; Lutz, M.; Gaillard, J.; Noodleman, L. *Biochemistry* **1988**, *27*, 8712–8719. (b) Przysiecki, C. T.; Meyer T. E.; Cusanovich M. A. *Biochemistry* **1985**, *24*, 2542–2549.
(34) Sola, M.; Cowan, J. A.; Gray, H. B. *J. Am. Chem. Soc.* **1989**, *111*, 6627–6630.
(35) Meyer, T. E. *Biochim. Biophys. Acta* **1985**, *806*, 175–183.
(36) Moulis, J.-M.; Meyer, J. *Biochemistry* **1982**, *21*, 4762–4771.
(37) Banci, L.; Bertini, I.; Luchinat, C.; Piccioli, M.; Scozzafava, A.; Turano, P. *Inorg. Chem.* **1989**, *28*, 4650–4656.
(38) Johnson, R. D.; Ramaprasad, S.; La Mar, G. N. *J. Am. Chem. Soc.* **1983**, *105*, 7205–7206.
(39) Inubushi, T.; Becker, E. D. *J. Magn. Reson.* **1983**, *51*, 128–133.
(40) Vold, R. L.; Waugh, J. S.; Klein, M. P.; Phelps, D. E. *J. Chem. Phys.* **1968**, *48*, 3831–3832.
(41) (a) Bertini, I.; Luchinat, C. *NMR of Paramagnetic Molecules in Biological Systems*; Benjamin-Cummings: Menlo Park, CA, 1986. (b) Banci, L.; Bertini, I.; Luchimat, C. *Nuclear and Electron Relaxation*; VCH Publishers Inc.: Weinheim, Germany, 1991.
(42) Davis, D. G.; Bax, A. *J. Magn. Reson.* **1985**, *64*, 533–535.
(43) Wider, G.; Macura, S.; Kumar, A.; Ernst, R. R.; Wüthrich, K. J. *J. Magn. Reson.* **1984**, *56*, 207–234.
(44) Macura, S.; Wüthrich, K. J.; Ernst, R. R. *J. Magn. Reson.* **1982**, *47*, 351–357.
(45) Duben, A. J.; Hutton, W. C. *J. Magn. Reson.* **1990**, *88*, 60–71.

respectively. 2D EXSY spectra[46,47] were obtained using the standard phase sensitive pulse sequence, 4 ms for the mixing time, 660 experiments in the f_1 dimension, 360 scans per experiment, repetition time 150 ms, and 2K data points in the f_2 dimension. 2D TOCSY spectra were recorded with the RD–90–t_1–SL–MLEV17–SL–90 –AQ pulse sequence, where SL denotes a spin lock field applied for a short time along the x axis and MLEV17 is a composite pulse sequence.[48] A repetition time of 500 ms, a mixing time of 40 ms, and 800 experiments performed in the f_1 dimension with 128 scans per each experiment and 1K data points in the f_2 dimension were used.

For all 2D spectra, the data matrix was multiplied by a phase-shifted squared sine bell window function in both dimensions, prior to Fourier transformation. A standard Bruker software package was used for data processing.

Results

The procedure used to perform the selenium-for-sulfur substitution in the HiPIP II from *E. halophila* followed essentially the scheme already reported for the incorporation of the selenium cluster in the *C. vinosum* HiPIP,[34,36] the only difference being the much faster rate of cluster destruction by acid treatment than in the latter case.

The visible absorption spectra of the reduced and oxidized forms of **3**, shown in Figure 1A, were very similar to those of **4** already reported.[33a] As in the case of **4**, in the present case the bands are rather ill-resolved but consistent with the already proposed small red shifts of the bands assigned as LMCT (ligand–metal charge transfer) with respect to the spectra of the native proteins. The reappearance of LMCT bands upon cluster reconstitution from the apoprotein confirms the incorporation of the selenium cluster.

The CD spectra of reduced and oxidized forms of **3** and **4** have also been recorded in an attempt to increase the resolution of the LMCT bands (Figure 1B and C). These spectra can be compared with those already reported for **1** and **2**.[33b] The reduced forms confirm a slight red shift for at least four bands. The oxidized form of **3** shows a rather large red shift for the band at ≈460 nm (≈420 nm in **1**), while lower energy bands are substantially unaffected. Comparison of the oxidized forms of **2** and **4** is less clear: in both cases many more bands than in the case of oxidized **1** and **3** are observed, and it is difficult to establish a safe correspondence between the two spectra.

The EPR spectrum of **3**, shown in Figure 2, is characterized by a pure axial signal with $g_\parallel = 2.198$ and $g_\perp = 2.046$. The spectrum of **4**, characterized by an almost axial signal ($g_1 = 2.168$, $g_2 = 2.034$, and $g_3 = 2.028$) and by the presence of additional features at apparent g values 2.152, 2.117, 2.085, and 2.055, has been previously reported.[33a] These spectra are respectively analogous to the spectra of **1**,[9] characterized by a single axial signal with $g_\parallel = 2.146$ and $g_\perp = 2.030$, and **2**,[33a,49,50] characterized by a predominant axial signal with $g_\parallel = 2.12$ and $g_\perp = 2.04$ and by additional features at apparent g values 2.108, 2.08, and 2.055. In all cases, a larger anisotropy and a shift of the EPR signals to lower fields is observed upon passing from sulfur to selenium.

Similar to the native *E. halophila* HiPIP II,[30] **3** displays a very slow electron self exchange rate around room temperature. As a consequence, the oxidized and reduced proteins should be studied completely independently.

***E. halophila* Se HiPIP II ^{1}H NMR: Pairwise Cysteine β-CH_2 Proton Assignment and Temperature Dependence of the Shifts.** The 600-MHz ^{1}H NMR spectra of oxidized and reduced **3** at pH 5.2 are reported in Figure 3A. Comparing these spectra with the one for **1**,[51] one can immediately observe that in the case of **3** the hyperfine-shifted cysteine methylene signals are larger, indicating increased paramagnetism.[41] This is also revealed by comparing the values of the longitudinal relaxation times T_1, given in Table

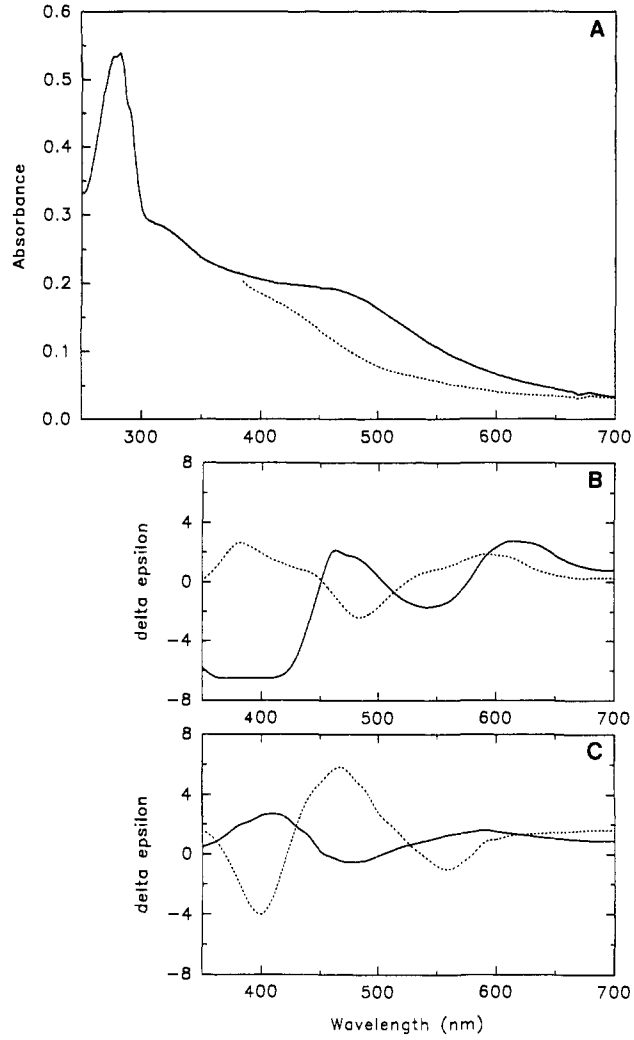

Figure 1. (A) UV–vis absorption spectra of oxidized (—) and reduced (---) **3**. (B) CD visible spectra of oxidized (—) and reduced (---) **3**. (C) CD visible spectra of oxidized (—) and reduced (---) **4**. The spectra were recorded on protein solutions in P_i 30 mM, pH 5.2.

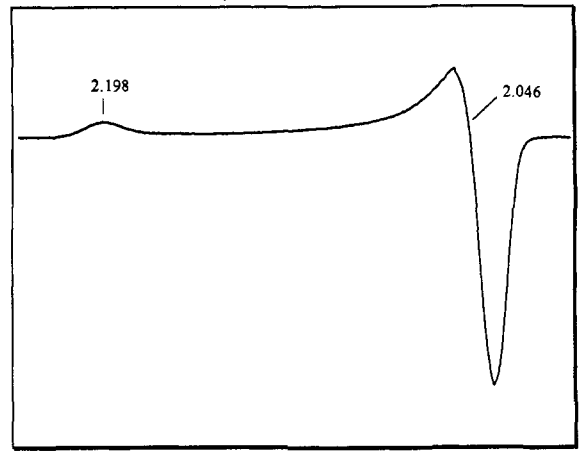

Figure 2. EPR spectrum (9.44 GHz) of oxidized **3**. The spectrum was recorded on a solution of the protein in P_i 30 mM, pH 5.2.

(46) Bodenhausen, G.; Ernst, R. R. *J. Am. Chem. Soc.* **1982**, *104*, 1304–1309.

(47) Ernst, R. R.; Bodenhausen, G.; Wokaun, A. *Principles of Nuclear Magnetic Resonance in One and Two Dimensions*; Oxford University Press: London, 1987.

(48) Bax, A.; Davis, D. G. *J. Magn. Reson.* **1985**, *65*, 355–360.

(49) Antanaitis, B. C.; Moss, T. H. *Biochim. Biophys. Acta* **1975**, *405*, 262–279.

(50) Dunham, W. R.; Hagen, W. R.; Fee, J. A.; Sands, R. H.; Dunbar, J. B.; Humblet, C. *Biochim. Biophys. Acta* **1991**, *1079*, 253–262.

(51) Banci, L.; Bertini, I.; Briganti, F.; Scozzafava, A.; Vicens Oliver, M.; Luchinat, C. *Inorg. Chim. Acta* **1991**, *180*, 171–175.

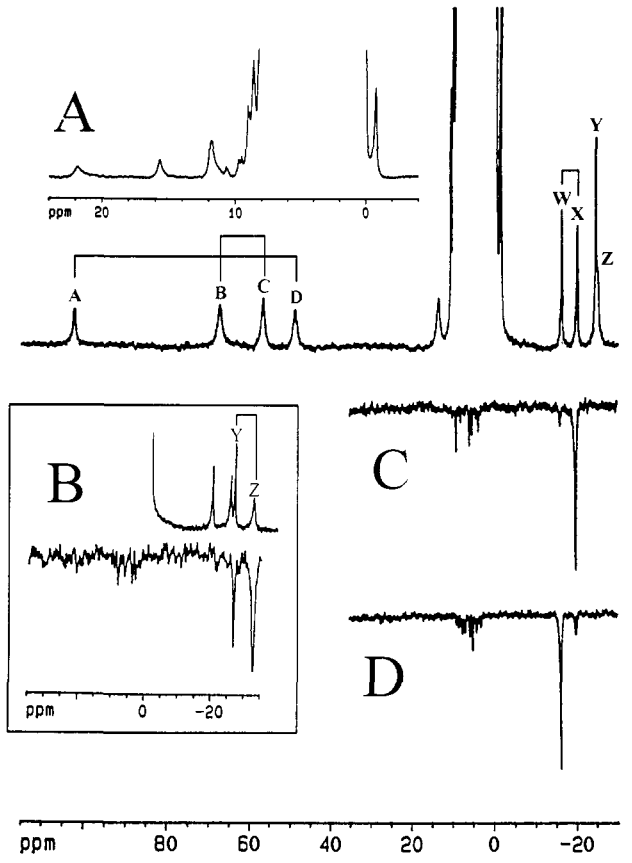

Figure 3. ^1H NMR spectra (600 MHz) of Se-substituted *E. halophila* HiPIP in D_2O, P_i = 30 mM, pH 5.2*: (A) reference spectra of reduced and oxidized protein at 298 K; (C and D) steady-state NOE difference spectra obtained by saturating peaks X and W, respectively. The upfield part of the reference spectrum at 285 K and the NOE difference spectrum obtained by saturating signal Z are reported in the inset (B). The geminal connectivities found by NOE experiments for hyperfine shifted signals are indicated.

Table I. Summary of ^1H NMR Parameters for Oxidized Se HiPIP II from *E. halophila* (3)

cysteine label	proton	signal	chemical shift (ppm)[a]	T_1 (ms)	sequence specific assignment	pair assignment
Cys I	Hβ1	Z	-24.87	6.2		
	Hβ2	Y	-24.46	15.6	Cys 39	"ferric"
	Hα					
Cys II	Hβ1	C	56.55	1.5		
	Hβ2	B	67.23	0.9	Cys 42	"mixed
	Hα					valence"
Cys III	Hβ1	D	48.70	1.5		
	Hβ2	A	102.25	3.5	Cys 55	"mixed
	Hα					valence"
Cys IV	Hβ1	X	-19.92	13.8		
	Hβ2	W	-16.13	7.0	Cys 71	"ferric"
	Hα	R	5.83			

[a] Chemical shifts refer to the oxidized protein at pH* 5.2.

I for the oxidized form, with those observed for **1**.[51] In the latter case, the 2–7-ms range has been reported for the downfield signals A–D, whereas the 7–25-ms range was observed for the upfield signals W–Z.[51] This increased paramagnetism has also been observed in model compounds.[52]

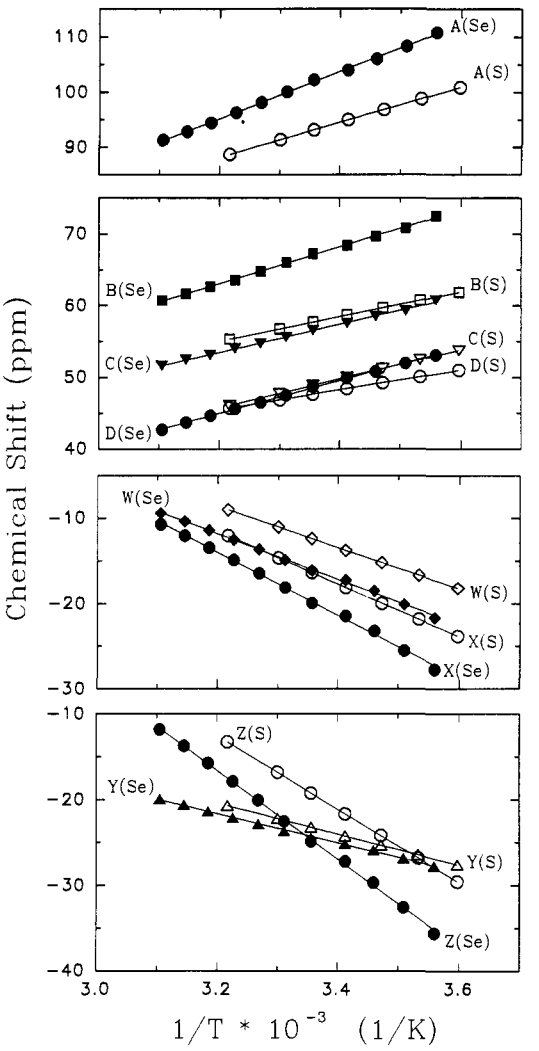

Figure 4. Temperature dependence of the hyperfine shifted signals of oxidized **1** (taken from ref 28) (empty symbols) and **3** (filled symbols).

In analogy with **1**, the reduced form shows four downfield-shifted signals. These signals in **1** were tentatively assigned by analogy with the reduced forms of other HiPIPs.[29] The analogy can be extended to **3** given the strong similarity of the spectra. Similar considerations may hold for the oxidized form. In this case, however, an independent assignment is carried out.

To establish the pairwise assignment of the hyperfine shifted signals to the four cysteine residues, a series of NOE experiments were performed (Figure 3B–D). The difference NOE experiment on signal Z (performed at 285 K because the signals Y and Z are almost degenerate at 298 K) indicated the connectivity Y-Z (Figure 3B) and suggested their assignment as β-CH_2 protons of a cysteine which we label Cys I. In the early published work on **1**,[51] it was evaluated that the steady-state NOE effects in the native protein should be around 1–3% for the downfield signals. Taking into account that **3** is more paramagnetic than **1**, we expected that, in the latter case, the observation of pairwise correspondences for downfield signals in NOE experiments would be almost impossible. In fact, the NOE difference spectrum obtained upon saturation of signal B showed a barely observable negative peak in correspondence of signal C (not shown). Thus, signals B and C belong to the same cysteine, Cys II. The difference NOE spectrum obtained upon saturation of signals W and X (Figure 3C,D) revealed the W–X connectivity (Cys IV). The connectivity A–D (Cys III) was thus established by exclusion. The pairwise assignment of the cysteine β-CH_2 pairs is reported in Table I.

(52) (a) Bobrick, M. A.; Laskowski, E. J.; Johnson, R. W.; Gillum, W. O.; Berg, J. M.; Hodgson, K. O.; Holm, R. H. *Inorg. Chem.* **1978**, *17*, 1402–1410. (b) Yu, S.-B.; Papaefthymiou, G. C.; Holm, R. H. *Inorg. Chem.* **1991**, *30*, 3476–3485.

(53) Gaillard, J.; Albrand, J. P.; Moulis, J. M.; Wemmer, D. E. *Biochemistry* **1992**, *31*, 5632–5639.

(54) Cowan, J. A.; Sola, M. *Biochemistry* **1990**, *29*, 5633.

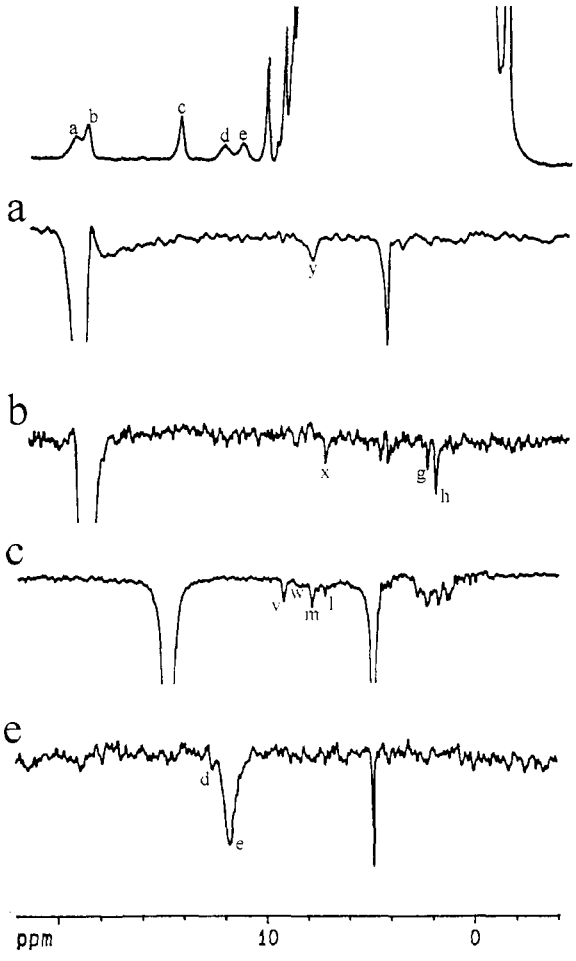

Figure 5. ^{1}H NMR spectra (600 MHz, 298 K) of reduced **4** recorded in D_2O, P_i = 30 mM, pH* 7.15: upper trace, reference spectrum. The NOE difference spectra are labeled according to which signal is saturated.

We then investigated the temperature dependence of signals corresponding to β-CH_2 cysteine protons. In the case of reduced **3**, the temperature dependence of the hyperfine shifted signals revealed a linear, anti-Curie behavior, explained in terms of an antiferromagnetic spin ladder, in which the excited, more paramagnetic levels become more populated as the temperature is increased. The chemical shift increments observed for the most shifted signals on passing from reduced **1** to **3** are 5 ppm (signal a), 3 ppm (signal b), and 1.5 ppm (signal c). As noted above, the sequence-specific assignment in this case cannot be performed by saturation transfer experiments due to the slow rate of exchange between the reduced and oxidized forms of the protein. Hyperfine shifted signals of oxidized **3** show the same temperature-dependence behavior as the corresponding signals in the native protein (Figure 4): downfield signals (A, B, C, and D), corresponding to Cys II and Cys III, move upfield with increasing temperature, whereas upfield signals (W, X, Y, and Z), corresponding to Cys I and Cys IV, move downfield with increasing temperature. Therefore, according to the above-discussed S_{34}, S_{12} coupling scheme, one can conclude that, as in **1**,[51] also in **3** the four downfield signals belong to cysteine residues attached to iron ions with "mixed-valence" character, while upfield signals correspond to cysteines bound to the "ferric" pair. The slopes of the downfield signals in **3** are more increased with respect to the corresponding slopes in **1** than is the case for the upfield signals. No marked deviations from linearity are observed.

***C. vinosum* Se HiPIP ^{1}H NMR: Pairwise Cysteine β-CH_2 Proton Assignment and Temperature Dependence of the Shifts.** The 600-MHz ^{1}H NMR spectrum of reduced **4** is shown in Figure 5, whereas the spectrum of the oxidized form is shown in Figure 6. These spectra reproduce exactly those previously reported.[34]

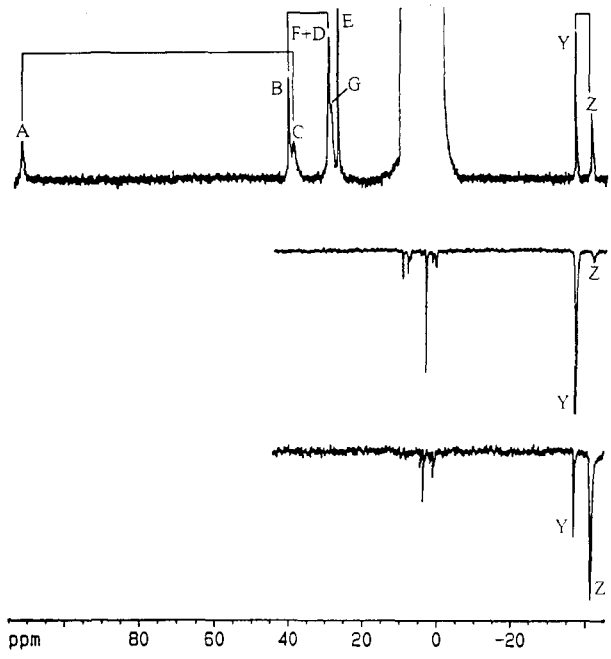

Figure 6. ^{1}H NMR spectra (600 MHz, 298 K) of oxidized **4**: upper trace, reference spectrum; lower traces, NOE difference spectra obtained by saturating sugnals Y and Z, respectively. The connectivities between cysteine geminal protons established by NOE and saturation transfer experiments are given.

Signals a–e are the isotropically shifted signals of the reduced form, whereas signals A–G, Y, and Z are the isotropically shifted signals of the oxidized form. These signals are in general more isotropically shifted with respect to the corresponding spectra of **2**,[14,26,27,53,54] although the pattern is unchanged. ^{1}H NOE experiments on the reduced and oxidized forms of **4** at pH 7.15, and 1D and 2D saturation transfer experiments on a 50% mixture of reduced and oxidized **4** at pH 5.2, were carried out to establish, on the one hand, the connections between the β-CH_2 proton pairs belonging to the same cysteine residue and, on the other hand, the correspondence between the signals of the two redox forms of the protein. The exchange rate between these two forms allows both the simultaneous observation of all the signals of the semireduced protein and the observation of the saturation transfer peaks. Saturation transfer on signals A, Y, and Z revealed that the corresponding signals of the reduced form are b, y, and a, respectively (Figure 7). An EXSY experiment (Figure 8) further confirmed the relationship Y–y, and showed the correspondences *B*–*c*, F–e, G–d, D–w, and E–v. The EXSY connectivity for signal C was not observed, perhaps as a consequence of the short T_1 for this signal (1.7 ms), which is the smallest of all the hyperfine shifted signals of the oxidized protein.[34]

The difference spectrum obtained upon saturation of signal a (Figure 5a) showed an NOE peak at 8.41 ppm, corresponding to signal y, also obtained upon saturation transfer of signal Y in the semireduced protein (Figure 7). The assignment for Cys I is thus reported in Table II. This assignment was confirmed by the presence of NOE connectivities between signals Y and Z in the oxidized protein (Figure 6).

The difference NOE spectrum obtained upon saturation of signal c (Figure 5c) showed three most evident peaks: v (9.26 ppm), m (7.85 ppm), and l (7.20 ppm), in addition to a broad peak w (8.2 ppm). Signal w was assigned to the β-CH_2 proton of the pair, on the basis of its large line width and on the basis of the presence of an EXSY cross peak between w and D (Figure 8). The difference NOE spectrum obtained upon saturation of signal c at higher temperature (303 K) (not shown) indicated that signal *w* is now too broad to be detected and, among signals v, m, and l, only signal v shows an anti-Curie behavior. This type

Figure 7. ^1H NMR spectra (600 MHz, 298 K) of an approximately 50/50 mixture of oxidized and reduced forms of **4**: upper trace, reference spectrum; lower traces, saturation transfer experiments establishing the correspondences of hyperfine shifted signals in the oxidized and reduced form of **4**. The correspondences A–b, Y–y and Z–a are presented.

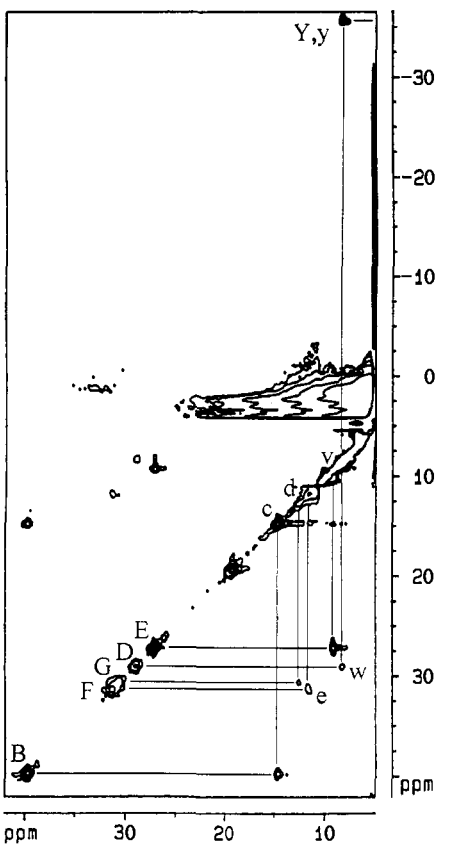

Figure 8. ^1H NMR EXSY spectrum (600 MHz, 298 K) of a sample containing approximately equal amounts of the oxidized and reduced forms of **4**. The connectivities between proton signals in the oxidized and reduced forms are reported. Conditions of the acquisition of the spectrum are described in the Experimental Section.

of temperature dependence indicates that signal v experiences some hyperfine shift, and it was thus assigned to the α-CH proton of the cysteine to whom signals c and w also belong. Signals E and D (which give an EXSY connectivity with signals v and w, respectively) were then assigned to the corresponding α-CH and β-CH_2 protons in the oxidized form of **4**. Signals m and l presumably belong to diamagnetic residues close to that cysteine residue. The full assignment of Cys IV is then established, and it is reported in Table II.

Signals d and e were assigned to the β-CH_2 protons of the same cysteine. In fact, a difference NOE experiment performed by saturating signal e (Figure 5e) revealed a very weak negative peak in correspondence with signal d. The weakness of this effect may be the consequence of the close proximity of the two peaks and of their large line widths and short T_1's (1.1 and 1.3 ms, respectively[34]). The assignment for Cys II is thus obtained, and it is given in Table II.

Finally, the difference NOE spectrum obtained upon saturation of signal b (Figure 5b) showed three major peaks: x (7.73 ppm), g (2.78 ppm), and h (2.37 ppm). Comparing this NOE pattern with the corresponding spectrum obtained by saturating signal b in **2**,[14] and considering the increased paramagnetism in **4**, one can conclude that signal z, observed in **2**, corresponding to the geminal β-CH_2, is now too broad to be observed, while signals x, g, and h, also present in the difference NOE spectrum of **2**,[14] are then assigned to diamagnetic residues spatially close to the β-CH_2 proton corresponding to signal b. Signal C is assigned as the geminal proton of signal A both by exclusion and by comparison with the assignment of the native protein. The assignment for Cys III is reported in Table II.

The previously reported[34] temperature dependence of the isotropic shifts of the signals belonging to the geminal methylene protons of the cysteine residues bound to the oxidized four-iron core in **4** has been more accurately redetermined in order to have a more reliable set of data to use for a simulation of the observed patterns and to draw conclusions on the difference in electronic distribution in the cluster cores in **2** and in **4**.

Hyperfine shifted signals of oxidized **4** show the same behavior as the corresponding signals in the native protein: signals A, B, C, and D, corresponding to Cys III and Cys IV, increase the resonant magnetic field with increasing temperature, whereas signals F and G, corresponding to Cys II, and upfield-shifted signals Y and Z, corresponding to Cys I, decrease the resonant magnetic field with increasing temperature (Figure 9).

Therefore, one can conclude that, as in **2**, also in **4** cysteine residues III and IV are attached to iron ions with "mixed-valence" character, while cysteines I and II are bound to the "ferric" pair. The slopes of the signals corresponding to the "mixed-valence" pair in **4** are more increased with respect to the corresponding slopes in **2** than it is the case for the signals corresponding to the "ferric pair". Moreover, while the isotropic shifts do not change very much for signals corresponding to Cys I, Cys III, and Cys IV, a much larger shift is observed for the couple of signals F and G, corresponding to Cys II, on passing from **2** to **4**. Finally, all the signals of **4** show more or less marked deviations from linearity. In particular, signals A–D show an upward curvature, whereas signals F, G, Y, and Z show a downward curvature. Such behavior has been previously observed, in a more marked degree, only in the oxidized HiPIP from *Ectothiorhodospiza vacuolata*, for which a chemical equilibrium between two species differing for the distribution of electron density within the cluster core has been proposed.[31]

***E. halophila* Se HiPIP II ^1H NMR: Sequence-Specific Assignment of Cysteine Residues.** Following the pairwise assignment of the eight hyperfine shifted signals, the sequence-specific assignment of these four pairs to the four cysteine residues was

Table II. Summary of ^{1}H NMR Parameters for Se HiPIP from *C. vinosum* (4)

cysteine label	proton	signal (oxidized)	chemical shift (ppm) (oxidized)[a]	signal (reduced)	chemical shift (ppm) (reduced)[b]	sequence-specific assignment	pair assignment
Cys I	Hβ1	Y	−35.6	y	8.41		
	Hβ2	Z	−38.8	a	19.7	Cys 43	"ferric"
	Hα						
Cys II	Hβ1	F	31.3	e	11.8		
	Hβ2	G	30.6	d	12.7	Cys 46	"ferric"
	Hα						
Cys III	Hβ1	A	112.0	b	19.2		"mixed valence"
	Hβ2	C	39.6			Cys 63	
	Hα						
Cys IV	Hβ1	B	39.7	c	14.8		"mixed valence"
	Hβ2	D	29.0	w	8.2	Cys 77	
	Hα	E	27.1	v	9.26		

[a] Chemical shifts refer to the oxidized protein at pH* = 5.2. [b] Chemical shifts refer to the reduced protein at pH* = 7.15.

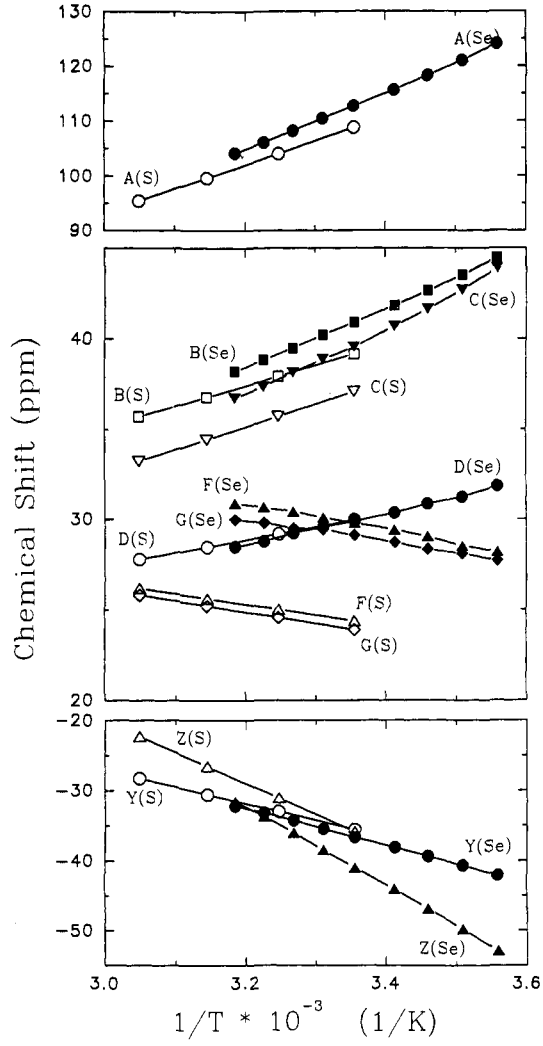

Figure 9. Experimental temperature dependence of the hyperfine shifted signals of oxidized **2** (taken from ref 34) (empty symbols) and **4** (filled symbols).

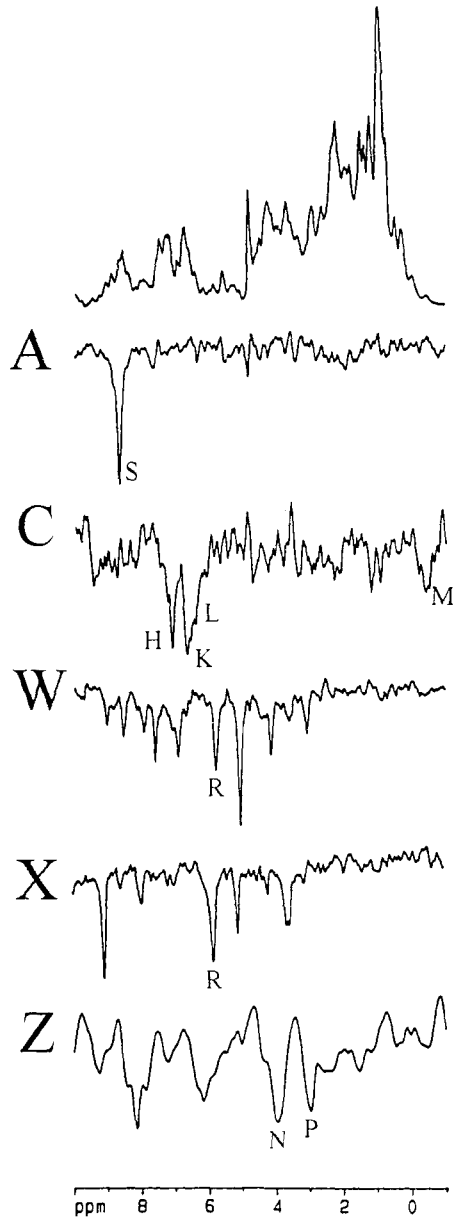

Figure 10. ^{1}H NMR spectra (600 MHz, 298 K) of the diamagnetic region of oxidized **3**: upper trace, reference spectrum; lower traces, NOE difference spectra labeled according to which signal is saturated. The NOE difference spectrum obtained by saturating signal Z was recorded at 285 K.

performed. Although in the present investigation 2D NMR experiments for **3** have not been carried out, the information necessary to complete the sequence-specific assignment was retrieved from a careful comparison of the diamagnetic regions of NOE difference spectra (Figure 10) obtained for **3** and for **1**.[30]

The spectrum obtained upon saturation of signal C (Figure 10C) (corresponding to signal D in **1**) showed signals H (7.15 ppm), K (6.72 ppm), L (6.50 ppm), and M (−0.41 ppm). This pattern reproduces exactly the difference NOE spectrum obtained when signal D is saturated in **1**, where the signals at 6.80 and 6.42 ppm (corresponding in **3** to K and L) were previously assigned to $C^{\epsilon}H$ and $C^{\delta}H$ of Tyr 74.[30] Thus, the pair of signals B–C can

Table III. Sequence-Specific Assignment (ppm) of Triptophane Residues in Reduced Se HiPIP from *C. vinosum* (**4**)

	$C^{\delta 1}H$	$N^{\epsilon 1}H$	$C^{\zeta 2}H$	$C^{\eta}H$	$C^{\zeta 3}H$	$C^{\epsilon 3}H$
Trp 60	7.30	10.20	7.55	7.30	7.42	7.21
Trp 76	6.85	9.85	7.52	6.70	6.90	7.20
Trp 80		10.70	7.42	6.97	7.20	7.43

be assigned to the Hβ2 and Hβ1 protons of Cys 42, respectively, as in the case of **1**.[30] This assignment is confirmed by the observation of signal H, because an analogous signal, at 7.55 ppm, has been observed upon saturation of both signals B and D of **1**.

Furthermore, signal Z gives NOE (this experiment was carried out at 285 K because at 298 K signal Z coincides with Y and the NOE experiment cannot be performed) with signals N (3.80 ppm) and P (2.93 ppm) (Figure 10Z). The position of these signals has not changed in comparison with NOE on signal Z for **1**, where they have been assigned as Hα1 and Hα2 of Gly 67, respectively. Residue Gly 67 lies close to the β-CH_2 protons of Cys 39. Therefore, we assign signals Z and Y as Cys 39 Hβ1 and Hβ2.

Upon saturation of signal A, a single signal S at 8.66 ppm is observed (Figure 10A), which corresponds to the single signal observed at 8.5 ppm upon saturation of signal A in **1**.[30] The pair A–D can thus be assigned to the geminal β-CH_2 protons of Cys 55, in analogy with the pair A–C in **1**.[30]

Finally, the NOE patterns observed when signals W and X are saturated (Figure 10W,X), are very similar to the corresponding patterns observed in **1**,[30] and they can thus be assigned to the geminal β-CH_2 of Cys 71. Furthermore, both signals W and X give NOE to signal R (5.83 ppm). Saturating W at 285 K, we observed that among all signals experiencing NOE, only R (now found at 4.03 ppm) shifted upfield with decreasing temperature (not shown). This behavior was observed also for signals W and X, so that signal R was assigned to the α-CH proton of Cys 71. Thus, as in **1**,[30] the correspondences Cys I–Cys 39, Cys II–Cys 42, Cys III–Cys 55, and Cys IV–Cys 71 are found for **3**, and the summary of the sequence-specific assignment of the eight methylene cysteine protons is presented in Table I.

***C. vinosum* Se HiPIP ^{1}H NMR: Sequence-Specific Assignment of Cysteine Residues.** The sequence-specific assignment of the cysteine signals was mainly performed by comparing the difference NOE patterns obtained in **2**[14,26] and in **4** (Figures 5 and 6). In fact, the patterns observed by saturating signals a–c, Y, and Z in **4** are entirely analogous to those observed by saturating the corresponding signals in the reduced[14] and oxidized[26] forms of **2**. This is a strong indication that the amino acid residues surrounding the β-CH_2 protons corresponding to the indicated signals are the same in the substituted and nonsubstituted forms of the protein. Thus, as in **2**,[26] the correspondences Cys I–Cys 43, Cys II–Cys 46, Cys III–Cys 63, and Cys IV–Cys 77 are found for **4** and are reported in Table II.

The conclusions drawn from this approach were confirmed, in some cases, by finding further connectivities in the NOESY and TOCSY maps of the reduced form of **4**. To accomplish this goal, it has proven useful to fully assign the signals belonging to the three Trp residues found in the protein.[55-57] This assignment was performed by looking at NOESY and TOCSY spectra of the reduced protein and following conventional methods.[58] The full assignments of Trp 60, Trp 76, and Trp 80 are reported in Table III. From the X-ray structure of the native HiPIP,[55-57] the α-CH proton of Cys 77 lies 2.77 Å from the $C^{\epsilon}H$ of Trp 76. In the NOESY map (not shown), a cross peak is observed between the $C^{\epsilon}H$ of Trp 76 (7.17 ppm) and signal v at 9.26 ppm, previously assigned as the α-CH of Cys IV. This connectivity confirms the Cys IV–Cys 77 assignment. Furthermore, Cys 63 Hβ2 is 1.75 and 3.49 Å from the Phe 66 Hβ1 and Hβ2, respectively. The NOE difference spectrum on signal b shows dipolar connectivities with the diamagnetic signals g (2.78 ppm) and h (2.37 ppm). Both in the NOESY and TOCSY maps, two cross peaks are observed between signals g and h, which are then assigned to a β-CH_2 pair. Among cysteine residues 43, 46, and 63, only Cys 63 Hβ2 lies close to the β-CH_2 pair corresponding to Phe 66, thus confirming the Cys III–Cys 63 assignment. The sequence-specific assignment for Se HiPIP from *C. vinosum* is reported in Table II.

Discussion

Structural studies on $[Fe_4Q_4]$ (Q = S, Se) model complexes[52] have established that when sulfur is substituted with selenium, the Fe–Q distances increase by about 0.12 Å, the Fe–Fe distances increase by about 0.05 Å, and the Fe–Q–Fe angles decrease by about 3°, due to the larger ionic radius of Se^{2-} with respect to S^{2-}. To elucidate the effect of these structural variations on the electronic structure of HiPIP, we have investigated the electronic properties of the selenium-substituted *E. halophila* HiPIP II. The choice of this protein derived from the fact that the EPR spectrum of its native counterpart, characterized by a single axial species,[9] does not show any complications due to intrinsic heterogeneity of the $S = {}^1/_2$ ground state, a phenomenon observed, instead, in the EPR spectra of several other HiPIPs.[31,49,50,59]

The effect on the EPR spectra of Se-for-S replacement in iron–sulfur proteins is difficult to predict.[60] For example, in [2Fe–2S] proteins, incorporation of selenium causes, in general, a shift of EPR signals to lower fields,[61-63] but the effect on the anisotropy can be different. For instance, in the case of putidaredoxin, the total anisotropy is increased[61] ($g_{\|} = 2.01$, $g_{\perp} = 1.93$, $g_{av} = 1.96$ for native protein and $g_z = 2.04$, $g_y = 1.98$, $g_x = 1.93$, $g_{av} = 1.98$ for selenium-substituted protein), whereas for parsley ferredoxin[63] the effect is opposite ($g_z = 2.052$, $g_y = 1.959$, $g_x = 1.899$, $g_{av} = 1.970$ for native protein and $g_z = 2.061$, $g_y = 1.965$, $g_x = 1.937$, $g_{av} = 1.988$ for selenium substituted protein). In models and proteins containing the $[Fe_4Q_4]^{1+}$ core, for which $S = {}^1/_2$, the presence of selenium causes a shift of the EPR signals to lower fields as well.[52a,64] For example, in the case of native ferredoxin from *Clostridium pasteurianum*, the $S = {}^1/_2$ state is characterized by g values of $g_z = 2.056$, $g_y = 1.925$, and $g_x = 1.883$, with $g_{av} = 1.956$, while for the Se derivative, the corresponding values are 2.103, 1.940, 1.888, and 1.979, respectively. Also, in some cases, EPR features indicative of the presence of higher spin ground states are observed.[64] In the EPR spectrum of **4**, containing the $[Fe_4Se_4]^{3+}$ cluster core, an increase of the anisotropy and number of detectable features due to additional doublet-spin ground states has been observed, together, again, with a shift of the EPR features to lower fields.[33a]

Various models have been proposed to interpret EPR spectra of exchange coupled systems.[65,66] According to these models,

(55) Carter, C. W., Jr.; Kraut, J.; Freer, S.; Alden, R. A. *J. Biol. Chem.* **1974**, *249*, 4212–4225.
(56) Freer, S. T.; Alden, R. A.; Carter, C. W., Jr.; Kraut, J. *J. Biol. Chem.* **1975**, *250*, 46–54.
(57) Carter, C. W., Jr.; Kraut, J.; Freer, S. T.; Alden, R. A. *J. Biol. Chem.* **1974**, *249*, 6339–6346.
(58) Wuthrich, K. *NMR of Proteins and Nucleic Acids*; John Wiley: New York, 1986.
(59) (a) Beinert, H.; Thomson, A. J. *Arch. Biochem. Biophys.* **1983**, *222*, 333–356. (b) Sweeney, W. V.; Rabinowitz, J. C. *Annu. Rev. Biochem.* **1980**, *49*, 139–161.
(60) Meyer, J.; Moulis, J. M.; Gaillard, J.; Lutz, M. *Adv. Inorg. Chem.* **1992**, *38*, 73–115.
(61) Tsibris, J. C. M.; Namtvedt, M. J.; Gunsalus, I. C. *Biochem. Biophys. Res. Commun.* **1968**, *30*, 323–327.
(62) Orme-Johnson, W. H.; Hansen, R. E.; Beinert, H.; Tsibris, J. C. M.; Bartholomaus, R.C.; Gunsalus, I. C. *Proc. Natl. Acad. Sci. U. S. A.* **1968**, *60*, 368–372.
(63) Fee, J. A.; Palmer, G. *Biophys. Biochim. Acta* **1971**, *245*, 175–195.
(64) (a) Gaillard, J.; Moulis, J. M.; Auric, P.; Meyer, J. *Biochemistry* **1986**, *25*, 464–468. (b) Moulis, J. M.; Auric, P.; Gaillard, J.; Meyer, J. *J. Biol. Chem.* **1984**, *259*, 11396–11402.
(65) George, S. J.; Thomson, A. J.; Crantree, D. E.; Meyer, J.; Moulis, J. M. *New J. Chem.* **1991**, *15*, 455–465.

the anisotropy of the **g** tensor is largely due to the variations of the coordination geometry around the reduced iron ions. In fact, the **g** tensor of the high-spin ferric ions is almost insensitive to variations of their coordination geometry because their electronic state is derived from the ^6S free ion configuration. On the other hand, the local g values of the high-spin ferrous ions increase with decreasing ligand field strength. The weaker coordination properties of selenide ions, as compared to sulfide ions, can thus explain the differences observed in the EPR spectra of **3** (Figure 2) and of **1**.[9] Furthermore, in the spectrum of **3** no signals indicative of the presence of higher spin ground states were observed.

In synthesis, we can conclude that the Se-for-S substitution does not influence markedly the properties of the spin ground state, because the J values remain large enough as to keep the ground spin state well isolated from excited states.

To verify this hypothesis, we have performed a study of the temperature dependence of the ^1H NMR spectra of reduced and oxidized **3** and **4**. The reduced form has been considered first, because it does not have the further complication of one pair of iron ions being different from the other pair. Thus the number of parameters in the problem decreases in the S_{34}, S_{12} coupling scheme discussed in the introduction, which has been used to simulate the experimental behavior. The first observation is that the isotropic shifts increase only about 1–5 ppm on passing from **1** to **3**. This is a confirmation that the ground spin state is still $S = {}^1/_2$. Moreover, the slope is very similar to the one observed for **1**. We have previously shown[12,14] that the temperature dependencies of the hyperfine shifts in reduced HiPIPs can be qualitatively reproduced by using the set of energies given by eq 1, with J_S on the order of a few hundred wavenumbers and ΔJ_{12} and ΔJ_{34} around $-{}^1/_3 J_S$. Values of $J_S = 300$ cm^{-1} and ΔJ_{12} and $\Delta J_{34} = -0.33 J_S$ can be used as reference values[12,14] for the sake of the following discussion. The slightly larger hyperfine shifts of **3** can then be reproduced using a smaller $J_{Se} \cong 0.8 J_S$, with again $\Delta J_{12} = \Delta J_{34} = -0.33 J_{Se}$.

The temperature dependence of the signals of the oxidized form of **3** can now be compared with the corresponding pattern observed for **1**. The latter can be, again qualitatively, reproduced with J_S on the order of a few hundred wavenumbers, $\Delta J_{12} = 0.33 J_S$, and either B_{34} on the same order of J_S or $\Delta J_{34} = -0.33 J_S$. If we take the same J_S value used for the reduced protein as a reference value we can reproduce oxidized **1** with $J_S = 300$ cm^{-1} and $\Delta J_{12} = -\Delta J_{34} = 0.33 J_S$. Trying to reproduce the behavior of oxidized **3** using the same coupling scheme and $J_{Se} = 0.8 J_S$, in analogy with the case of the reduced form, we notice that a satisfactory pattern is obtained by using $\Delta J_{12} = 0.33 J_{Se}$ and $\Delta J_{34} = -0.4 J_{Se}$. A more negative ΔJ_{34} value (or, equivalently, a larger B_{34} value) seems to be needed to better reproduce the experimental pattern. This can be interpreted as being due to a relative increase of the importance of double exchange on the "mixed-valence" pair. This effect may be consistent with Heisenberg exchange being dominated by superexchange through the selenide ions, and hence slightly reduced, and double exchange being dominated by direct Fe–Fe orbital overlap, less sensitive to the S → Se substitution.

An interesting feature to be noted is the slight curvature of the temperature dependence of the hyperfine shifts of oxidized **4**. Such curvature is not observed for **1** and **2** and is barely observable for **3**. This is the second case of curvature among all the investigated HiPIPs. A marked curvature was also observed in the case of the oxidized HiPIP II from *E. vacuolata*.[31] In principle, six different "mixed-valence" pairs can be present, and six possible molecular states in equilibrium are thus possible. We have previously proposed[31,32] that with the only exception of *E. halophila* HiPIP II, which is virtually in one state, all other HiPIPs may be equilibrium mixtures of mainly two forms, in different percentages. These forms correspond to a state of the protein in which the "mixed-valence" pair is coordinated by Cys 63 and Cys 46, as in the *E. halophila* HiPIP II, and another state of the protein in which the "mixed-valence" pair is coordinated by Cys 63 and Cys 77, the latter being slightly thermodynamically favored. As a result, the signals of the cysteine belonging to the "ferric" pair but partly involved in the "mixed-valence" pair are downfield and anti-Curie (signals F and G in **2** and **4**). When the ratio between these two forms is close to 50/50, curvature in the temperature dependence of the shifts is expected and indeed observed in *E. vacuolata* HiPIP II.[31] If the curvature observed in the present data is interpreted in terms of equilibrium, then it should indicate that Se substitution changes the ratio between the two states of *C. vinosum* by a small amount in the direction of making it slightly closer to 50/50.

The observation of four markedly upfield shifted signals in both **1** and **3** indicates that Se substitution in *E. halophila* HiPIP II does not appreciably alter the strong preference for one of the two states.

The CD spectra of the oxidized forms of **1**–**4**[33b] (Figure 1) are also consistent with this picture: while the spectra of **1** and **3** show rather well-resolved bands (and clear indication of red shift for at least one of them), the spectra of **2** and **4** show many more bands, as it might be expected for equilibrium between two species, which would be slow on the short time scale of CD spectroscopy.

In summary, Se substitution teaches us that the main determinants for the valence distributions in the various HiPIPs are structural properties imposed by the protein matrices and not the properties of the cubanes themselves. Se substitution only causes modest alterations in the Heisenberg coupling constants, and these alterations are more or less uniformly distributed over the whole cluster core. The overall slight reduction in the average Heisenberg exchange coupling causes the shrinking of the whole energy level ladder without major alterations of the level order. In turn, this causes a modest increase in paramagnetism and, indirectly, contributes to make the two electronic states in equilibrium less different in energy.

Acknowledgment. A.D. thanks Bruker Spectrospin Italiana for a research fellowship. This research was partly financed by the Italian National Research Council.

(66) Hagen, W. R. *Adv. Inorg. Chem.* **1992**, *38*, 165–222 and references cited therein.